Mechanics of Advanced Composite Structures 2 (2014) 87– 96

Semnan University

Mechanics of Advanced Composite Structures

journal homepage: http://MACS.journals.semnan.ac.ir

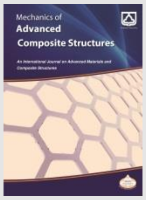

In Situ Formation of SiC/CNT Ceramic Nanocomposite by Phenolic Pyrolysis

H.R. Salehi*, M. Salehi

Department of Mechanical Engineering, Amirkabir University of Technology, Tehran, Iran

PAPER INFO

Paper history:
Received 12 June 2014
Received in revised form 26 September 2014
Accepted 29 September 2014

Keywords:
In situ formation
CNT
Nanocomposite
Silicon particles
Pyrolysis

ABSTRACT

In this research, using pyrolysis of phenolic resin in the presence of silicon particles, the SiC ceramic composite is formed. The samples were prepared by introducing 30, 35, 40, 45 and 50 wt% of Si particles to the phenolic resin. The samples were cured at 180°C then carbonized at 1100°C. The final carbonized C/Si composites are hot-pressed at 1500°C in inert atmosphere, which is more than the melting point of Si particles. In this temperature, Carbon vapor and melted Si react and SiC ceramic is formed. The XRD analysis of samples showed that SiC peak was observed in the final product while carbonized phenolic and Si particles also existed in the matrix. The samples were so brittle and therefore, several impregnation processes should have been used to reduce the porosity of composite. SEM images of in situ composite reveal extraordinary phenomenon which is related to the formation of CNT and nanostructures on the base of Si particles that grow like flower in the matrix. These nanostructures are one of the reasons for higher mechanical properties of final nanocomposite. Three-point flexural tests are also conducted for better understanding of mechanical improvement.

1. Introduction

Ceramic matrix and C/C composites are very important materials in the fields of aerospace, defense and other industries. These composites have very desirable high-temperature properties including high strength, high stiffness and low density [1]. These kind of composite materials are used in different applications like nose, nozzle, jet-vane, motor parts and other parts of shuttle, flying objects, aircrafts and airplanes, and power plants. There are many other emerging applications in common industries such as automobile, chemical and thermal industries such as brake disks, and heat insulating materials [2-5].

Phenolic resin is one of the main carbon precursors that can be used for fabrication of high temperature composites. The pyrolysis of phenolic matrix is a critical step in the manufacture of high temperature carbon/carbon components [6]. Trick and Saliba [6] try to understand the reaction kinetics of the pyrolysis reactions that is essential for advancement in the processing of carbon/carbon materials. They propose a mechanism for the pyrolysis of carbon/phenolic composites which describes the resin pyrolysis reaction as occurring in three major reaction regions: formation of additional crosslinks, breaking of the crosslinks, and stripping of the aromatic rings. The evolution of microstructure and properties of phenolic resin-based carbon/carbon composites during pyrolysis at different temperatures up to 2500°C was investigated by Tzeng and chr [7]. Results of weight loss and open porosity

---

[*] Corresponding author. Tel.: +98-21-22689652; Fax: +98-21-22673685

E-mail address: h.r.salehi@gmail.com

measurements and microstructure observations indicated that a rapid increase in porosity resulted from the decomposition of phenolic resin matrix below 600°C, whereas the cracks were developed mainly above 600°C. Atarian et al. [8] investigated the effect of TiC, SiC, TiO_2 and ZrO_2 nanoparticles on the tribological behavior of phenolic resin. This research showed that nanoparticles had improving effect on mechanical and wear properties. The optimum curing and carbonization cycles of phenolic resin were studied in [9-10].

Zawrah and Aly [11] prepared five composite batches containing Al_2O_3–SiC–mullite–Al that were designed in situ from different proportion mixtures of alumina, silicon carbide and aluminum alloy. The phase composition and microstructure were studied using X-Ray Diffraction (XRD) and Scanning Electron Microscope (SEM) techniques. Sinterability in terms of bulk density, apparent porosity and compressive strength were also measured. They understand that the formed mullite or silica rich phase prevents further oxidation of SiC or Al–metal. These phase compositions reflect the higher density, lower porosity and good mechanical properties of such composites. The presence of low melting silicate phases was found to increase the bulk density and consequently to decrease the apparent porosity.

D'angelo et al. [12] studied CO interaction with SiO_2/Si system at high temperature (~ 1100 °C) and 350 mbar by core-level photoemission. Even for short annealing time (5 min) the signal from Si2p and C1s core levels showed a clear change upon CO treatment. Shifted components were attributed to formation of SiC. This is confirmed by TEM imaging which further shows that the silicon carbide is in the form of nano-crystals of the 3C polytype.

In situ oxidation resistant and solid refractory coatings have been generated on 20 vol% SiC-reinforced ZrB_2 ultra high temperature ceramics containing 10 wt% rare earth (RE) additives such as LaB_6,La_2O_3, and Gd_2O_3 fabricated by spark plasma sintering [13]. Oxidation for 1 h at 1600°C in static air led to formation of a dense layer (up to 250 μm thick) of ZrO_2 and RE-zirconates on the composite systems underneath which were intermediate layers (50–100 μm) containing heterogeneous crystalline oxides such as $La_2Zr_2O_7$ and amorphous silicate phases.

Chung and Wu [14] investigated the effect of substrate temperature on the in-situ formation of crystalline SiC (c-SiC) nanostructured film using Ultra-High-Vacuum Ion Beam Sputtering (UHV IBS). The phase transformation, bonding behavior, morphology, composition and interdiffusion of the SiC nanostructured film were examined using X-ray diffraction, Raman spectra, high resolution Scanning Electron Microscopy (SEM) with the attached energy dispersive X-ray detector and Auger Electron Spectroscopy (AES) depth profile, respectively. The in-situ formation of c-SiC was through interdiffusion and reaction between the sputtered carbon (C) and the crystalline Si (c-Si) substrate at high temperature. The amorphous-like C microstructure was stable up to 500 degrees C and transformed into a new phase of c-SiC together with the remained C at 600 degrees C. Complete C and Si reaction was found at 700 degrees C from Raman spectra without any C peaks. The main diving force for the c-SiC formation was the thermal energy to activate the large interdiffusion between C and c-Si which was detected from AES depth profile. Also, a nanoweb-like morphology of the c-SiC was observed on the surface of film from the SEM image. Therefore, the c-SiC nanostructured film can be obtained at 700 degrees C using in-situ UHV IBS process, which is much lower than conventional CVD c-SiC.

Theoretical and experimental studies on the in-situ formation of an Al-Si alloy composite were carried out by Wu and Reddy using a methane gas mixture [15]. An Al-Si alloy composite with in-situ formed SiC as a reinforced phase was produced by bubbling methane gas at temperatures of 1223 to 1423 K. An optical microscope, Scanning Electron Microscope (SEM), and electron microprobe were used for the product characterization. Primary and eutectic silicon were observed in the samples taken from the top part of the crucible, and only eutectic silicon was observed in the samples taken from the bottom of crucible. The SiC formation rate increased with the decrease in the bubble size. A silicon concentration gradient existed at different vertical positions of the liquid alloy. The silicon concentration close to the top of the liquid alloy was higher than that at the bottom. The SiC concentration was very low in the bulk alloy. The bubbling of the gas mixture in the melting process resulted in the formation of a layer of foam on top of the crucible. Formed SiC particles were enriched in the foam and were carried out of the crucible by the overflow foam to a composite collector located under the crucible. The foam in the composite collector was broken, and composites in the foam contained up to 30 wt pct SiC. The particle size of the SiC was in the range of 1 to 10 μm. The bubbling process resulted in the unevenness of the silicon concentration and the different crystallizing processes.

Krishnarao et al. [16] synthesized composite powders of molybdenum silicide–SiC using reacting mixtures of (Mo–SiO_2 –C), (Mo–Si_3N_4 –C), and (Mo–SiO_2 –Si_3N_4 –C) powders at 1300 °C. In the (Mo–SiO_2

–C) system Mo_5Si_3 and Mo_3Si were formed predominantly. $MoSi_2$ formed the major constituent of the reaction product from powder mixtures containing Si_3N_4. Vapor-solid SiC whiskers were formed in the (Mo–SiO_2 –C) system. Vapor-liquid-solid whiskers of SiC and Mo_5Si_3C were formed in (Mo–SiO_2 –Si_3N_4–C) and (Mo–Si_3N_4 –C) systems, respectively. The mechanism of formation of the VLS whiskers and molybdenum silicides was identified as follows: initially a thin layer of Mo_2C was formed on Mo particle; the Si vapor from thermal decomposition of Si_3N_4 deposited on the Mo_2C surface and formed a droplet of ternary "Nowotny phase" $Mo<_5Si_3C<1$; an SiC/Mo_5Si_3C whisker was formed by nucleation and growth from the supersaturated ternary phase; after reaction with the Mo_2C layer, the SiO/Si vapor further reacted with Mo particle to form bulk silicides.

Oidia et al. [17] described a simple method to detect the formation of graphene during Si sublimation from SiC surfaces at elevated temperature. The method exploits differences in the thermionic emission current density between graphene and SiC. When graphene forms, the thermionic current from the sample increases by a factor of about 20. The increase in thermionic emission can be detected in situ using a biased plate located near the sample. The ability to detect when graphene forms during processing is useful in optimizing graphene synthesis processes.

An in situ reaction was proposed and investigated to produce Mo(Si1 − x Al x)2-SiC composites by Zhang et al. [18]. The starting powders were $MoSi_2$, Al and C. A Direct Current Hot Pressing (DCHP) method was used to prepare these composites. When the mixed powder was hot pressed at temperatures lower than 1500°C, the phase composition was $Mo(Si,Al)_2$ and β-SiC. When the hot pressing temperature was higher than 1600°C, however, Nowotny phase $Mo\leqq_5Si_3C\leqq 1$ appeared. The chemical stoichiometry of the proposed in situ reaction becomes difficult due to the formation of solid solution among these phases and the appearance of Mo_5Si_3C phase. The in situ formed SiC phase in the x = 0.3 sample was partly in whisker shape. However, the SiC phase in x = 0.15 sample was in particle shape. These in situ formed SiC particles and whiskers acted as crack deflection and bridging elements and improved the fracture toughness.

Carbon Nanotube (CNT) reinforced SiCf/SiC composite was prepared by in situ Chemical Vapor Deposition (CVD) growth of CNTs on SiC fibers then following Polymer Impregnation Pyrolysis (PIP) process in [19]. The nature of CNTs and the microstructure of the as prepared CNT–SiCf/SiC composite were investigated. The mechanical properties of the as prepared CNT–SiCf/SiC composite were measured. The results reveal that the in situ CVD growth of CNTs on SiC fibers remarkably promotes the mechanical properties of SiCf/SiC composite. The secondly pull-out of CNTs from matrix during the pull-out of the SiC fibers from matrix consumes the deformation energies, resulting in promotion of the mechanical properties ofcomposite.

The main purpose of present research is to show new method for synthesis of In-Situ formation of CNT/SiC nanocomposite with improved properties and optimization of process parameters for instance thermal cycle, filler percentage and mixing method. Detailed images of microstructures indicated in different stage of synthesis process helps a better understanding of undergoing phenomena and variation of microstructures.

2. Materials and Test Procedure

2.1. Synthesis of Phenolic Resin

Most of the commercial phenolic resins have low viscosity and cannot be used for fabrication of pyrolyzed composite. So, for fabrication of carbon matrix in the present work, a mixture of four items are used; they are novolac (Merck, Germany), hexamine (Merck, Germany), furfural and furfuryl alcohol (Merck, Germany) mixed with proper percentage and manner to produce phenolic resin with high and proper viscosity. Polymerization, solidification and optimum curing cycle are obtained by Salehi [20]. So, curing of the phenolic resin is performed in hot-stage press at 180 and a pressure of 10 MPa. After using the curing cycle which is shown in Fig. 1, the flexural test is conducted and the flexural strength and stiffness of the polymer are obtained.

2.2. Addition of Si Particles to Phenolic Resin

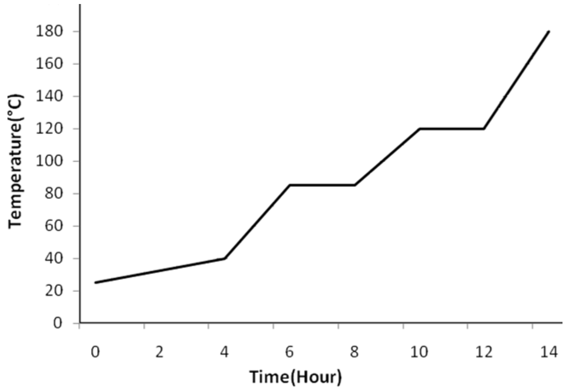

Figure 1. Phenolic resin polymerization cycle to obtain the optimum properties [9]

The properties of Si particles are shown in Table 1. As can be observed from SEM of Si particles in Figure 2, the size of particles is almost around 5-10 µm. The Si particles were added to Furfuryl Alcohol with different 30, 35, 40, 45 and 50 wt.% and were mixed ultrasonically about half an hour with power of 1200W and frequency of 20KHz.

The Si particles were added to Furfuryl Alcohol with different 30, 35, 40, 45 and 50 wt.% and were mixed ultrasonically about half an hour with power of 1200W and frequency of 20KHz. The obtained mixture was homogenized with Novolac, Hexamine and Furfural in proper procedure and portion [9]. Final mixture first cured at 180°C based on figure 1 and then carbonized with the optimum carbonization cycle of figure 3 were proposed by Salehi et al. [9].

The final carbonized samples were hot-pressed with the linear cycle at 1500°C with 30 MPa and duration of 20 hours in inert atmosphere based on the diagram of figure 4.

2.3. Three-Point Flexural Test

The dimensions of the samples for flexural test were 10cm×1cm×1cm and the test machine used was universal testing machine STM-400 (Santam, Iran). The crosshead speed was set to be 1mm/min.

Table 1. Properties of Si particles used for reinforcing carbon matrix.

Material	Mesh	Purity (%)	Code	Supplier
Si Powder	1500	99	SI-M-02-P	American elements, USA

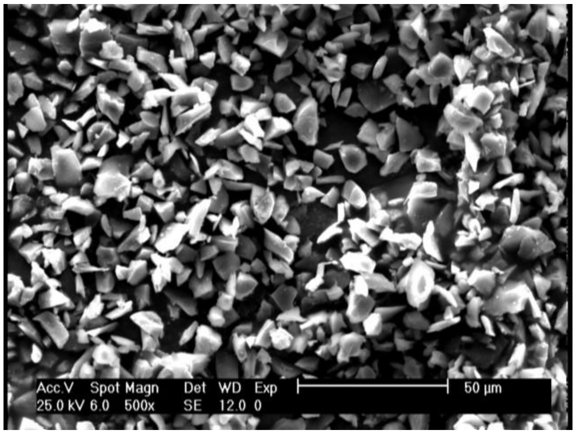

Figure 2. SEM Images of Si Particles

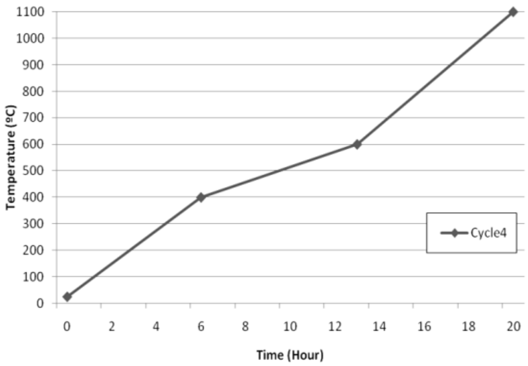

Figure 3. Optimum carbonization cycle that proposed by Salehi et al. [9]

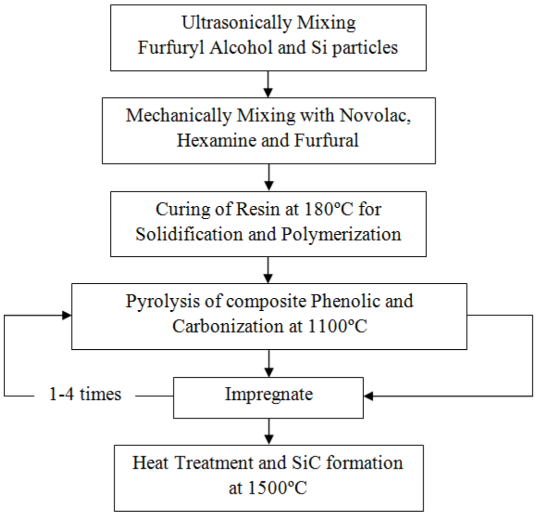

Figure 4. Curing, carbonization and heating diagram of Si/phenolic samples

The tests were carried out based on ASTM D790 [21]. Three-point flexural test was used instead of tensile test due to the brittleness and crushing behavior of samples. Figure 5 shows the sample and the fixture in three-point flexural test [9]. Figure 5, also, shows the samples during the three-point flexural test.

2.4. Scanning Electron Microscope (SEM) Imaging of Samples

For a better understanding of microstructure of samples and formation of possible micro or nano structures in the matrix, SEM imaging has been used in different stages of this research. The SEM used in this research was JOEL with magnification power of 100000X.

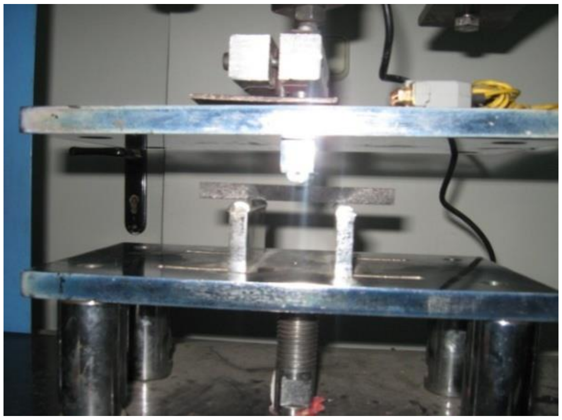

Figure 5. Three-point flexural test fixture for samples

3. Results and Discussion

3.1. Formation of SiC in Matrix

Synthesis of proper matrix in composite is very crucial for better resisting of yielded composite against the external, thermal, mechanical and chemical loading. The use of some active and inactive fillers can have improving influence on the final composite. However improper dispersion of fillers in the matrix can cause inhomogeneity and porosity of the matrix.

Inactive fillers have limited effect on the mechanical properties but good influence on the tribological and thermal behaviors. But active fillers cause better interaction and interfacial area between the matrix and filler and have so great effect on the behaviors.

The term of active or inactive can be described based on the reaction of filler during the synthesis process.

The melting point of Si powder is about 1414°C and therefore, in the heating cycle of 1500°C, the silicon is liquid. The carbon is also vaporized above 500°C. So, the possibility of SiC formation can be increased above 500°C. In presence of oxygen, Si oxidizes and forms SiO_2 and also carbon matrix can react with the oxygen molecules and forms CO_2. So it is very important to control the atmosphere of furnace during the heating and cooling procedure. The reaction of Si and carbon matrix is formulated as follows [6-7].

$$Si+C \rightarrow SiC \qquad (1)$$

Temperature around 1250°C- 1600°C in the Argon atmosphere.

$$3Si+2N_2 \rightarrow Si_3N_4 \qquad (2)$$

Temperature around 1300°C- 1400°C in the Nitrogen atmosphere.

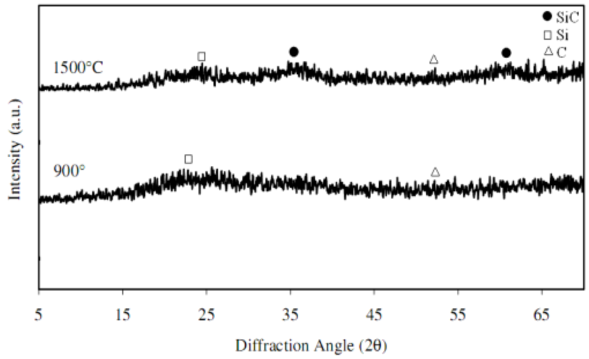

Figure 6. XRD analysis of matrix that shows formation of SiC phase

The XRD of carbonized Si/phenolic mixture before and after heating at 1500°C shows the formation of SiC phase in the matrix indicated in figure 6. The XRD shows the creation of new peaks in the curve that is related to SiC formation in the matrix. These peaks are observed in the 2θ=36º and 2θ=60º.

3.2. Density Variation of Samples

The density of samples before and after final heating process of 1500°C, is measured based on the procedure [22]. Table 2 shows the samples names, mixture and also density before and after the formation of SiC ceramic phase. As it is illustrated in table 2, MSi-45 has the highest value of density after the formation of SiC matrix and by increasing the Si content in the composite, the density of fabricated composite increases, which is predictable by rule of mixtures. However the porosity causes deviation from the linear trends.

3.3. SEM Imaging of Samples

The SEM image of carbonized phenolic without any filler and modification is illustrated in figure 7. The different shapes and sizes of porosity of carbon matrix are seen in the figure 7 (a) and 7 (b) that are formed due to pyrolysis process and volatile vapor of chemical reaction [10]. The fracture surface of carbonized phenolic resin shows several porosities in the microstructures that should be eliminated by impregnation of resin and repeating of curing and carbonization cycles. As it is obvious by comparison of figures 7 and 8, formation of SiC ceramic in the matrix changes the microstructure of the matrix. Some strong bonding can also be seen in the figure 9. The Si particles are bonded to each other and form 3D microstructure in composite but some porosity still exists in microstructures.

Table 2. The samples prepared from mixing Si and phenolic resin

Composite type	Si Content (Wt. %) (Vol. %)	Resin (%)	Density of resin (g/cm^3)	Density of ceramic (g/cm^3)
MSi-00	0	100	1.27	1.20
MSi-30	30(19)	70(81)	1.49	1.63
MSi-35	35(23)	65(77)	1.53	1.95
MSi-40	40(27)	60(73)	1.57	2.13
MSi-45	45(31)	55(69)	1.61	2.34
MSi-50	50(36)	50(64)	1.66	2.20

Figure 8 (b) indicates some particles with sharp edge and also some smaller semi-spherical particles.

3.4. Formation of Nanostructures in the Matrix

By profound investigation into the microstructure of samples, one extraordinary and interesting phenomenon is observed in the matrix. Because of the presence of Si particles in the matrix under high temperature of above 500°C, some nanostructures are formed in microstructures.

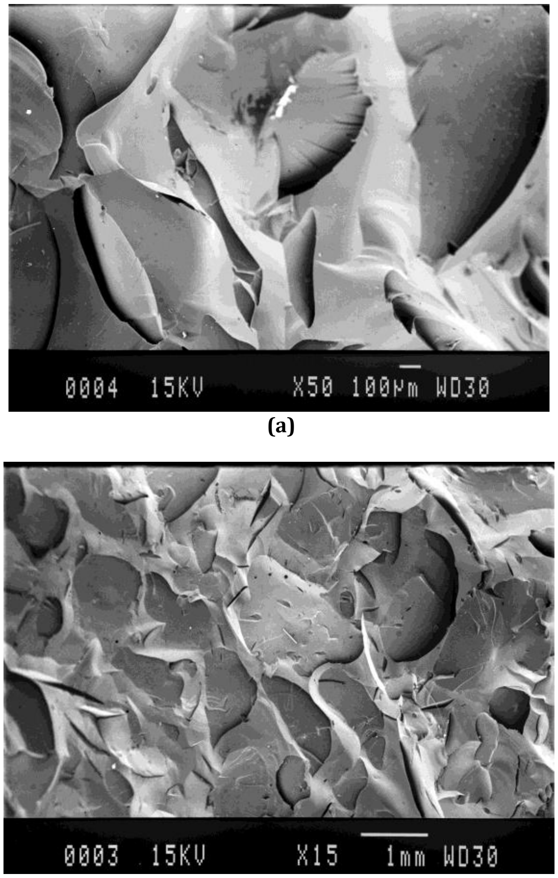

(a)

(b)

Figure 7. a) SEM Images of fracture surface of carbonized phenolic resin (50X) **b)** SEM Images of fracture surface of carbonized phenolic resin (15X)

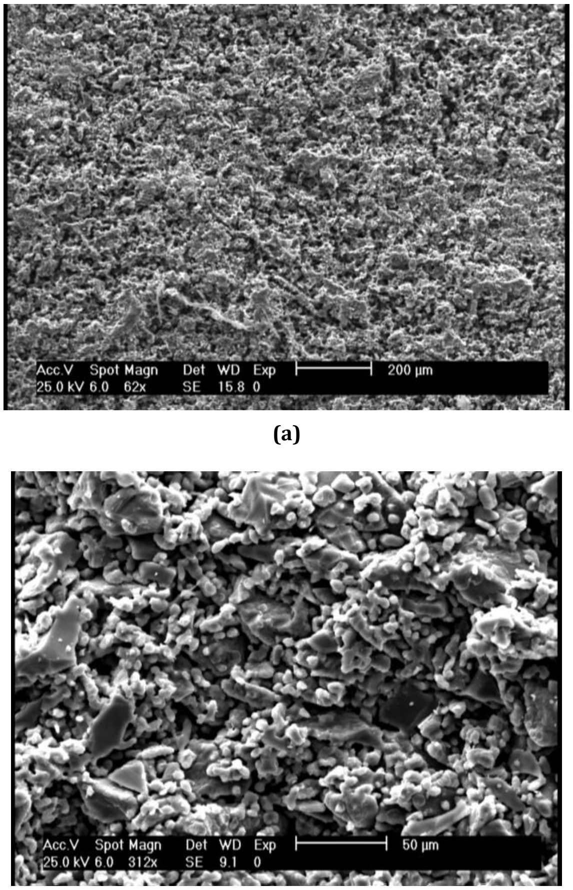

(a)

(b)

Figure 8. a) Microstructure of SiC ceramic matrix (MSi-45) after cycle 1500°C – (62X) **b)** Microstructure of SiC ceramic matrix (MSi-45) after cycle 1500°C – (312X)

These nanostructures that are formed during the thermal cycle, are in different sizes and morphologies. They are mostly in the form of flower-shape, tube and plates.

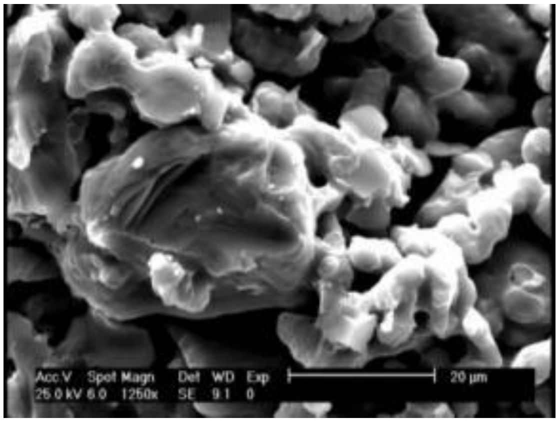

(a)

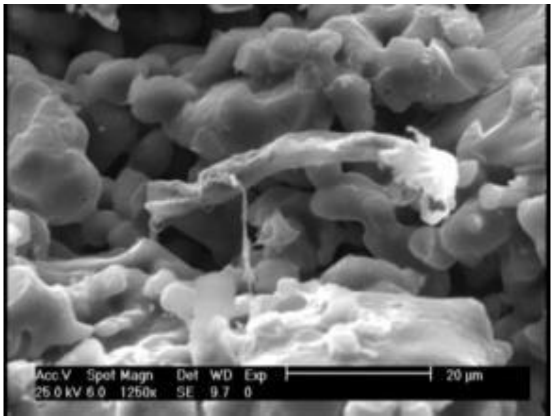

(b)

Figure 9. a) Strong bonding of Si particles and carbon matrix that forms SiC structures **b)** Strong bonding of Si particles and carbon matrix that forms SiC structures

The amount of nanostructure that is formed in matrix is not predictable because it is not added to the matrix but as a result of chemical reaction that might not be completely fulfilled. In this phenomenon, Si particles act as a catalyst and so vaporized carbon is formed as CNT and flower-shaped structures in the matrix. The SEM images show this phenomenon. Figures 10-15 show the formation of these nanostructures in the matrix. Figures 10 (a) and 10 (b) show some flower-shape nanostructures that are formed from the Si particle surface. The size of this nanostructure has been shown in figure 10 (a).

Figure 11 illustrates agglomeration of CNT nanostructures in the porosity of matrix. The diameter of CNT has been shown in figure 12. Figures 13-15 illustrate some nano plates in the nanocomposite structures that formation and exact compound require deeper insight to the chemical phenomena of nanocomposite synthesis.

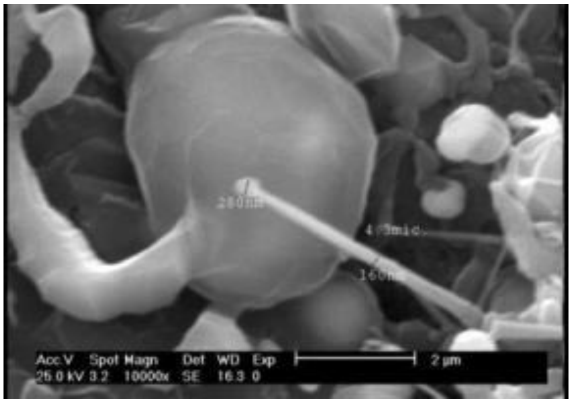

(a)

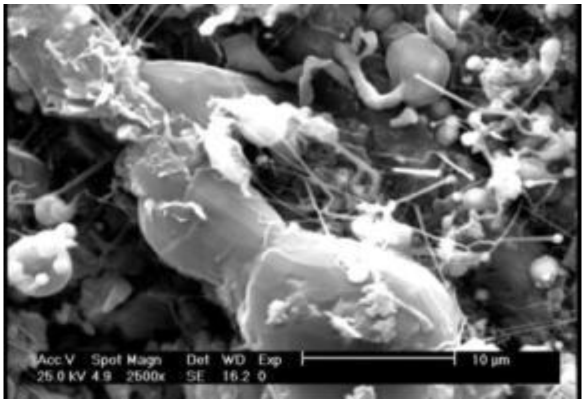

(b)

Figure 10. a) Flower-shaped nanostructures that formed in microstructures (10000X) **b)** Flower-shaped nanostructures that formed in microstructures (2500X)

Table 3. Three-point Flexural test results of Strength of samples before heating at 1500°C

Specimens	Average (MPa)	Variation (%)	Test 1 (MPa)	Test 2 (MPa)	Test 3 (MPa)
MSi-00	41.04	0	43.55	36.66	42.93
MSi-30	39.81	-3	38.5	35.10	45.83
MSi-35	45.12	+9	41.75	47.23	46.38
MSi-40	47.34	+15	42.74	48.03	54.27
MSi-45	45.5	+10	52.44	45.67	48.39
MSi-50	41.15	+0	38.59	41.6	43.26

3.5. Flexural Test Results

The three-point flexural test results are shown in Tables 3 and 4. Three samples are used for each case and the results show the average flexural strength of all the three samples. The flexural strength value is 41.04MPa for carbonized phenolic without any reinforcement.

Based on the test result, by adding Si into the carbon matrix before the final heating stage, the strength of the composite is improved slightly. This improvement is totally based on the inactive presence of Si particles in the matrix. And also these results show that in high percentages of Si in the matrix, the improvement is negligible. The average values of strength of phenolic resin are shown in Table 3. The results of samples after formation of the SiC in the matrix show that this formation has significant effect on the strength of the composite. This improvement is about 39, 48, 55, 70 and 60 percent for MSi-30, MSi-35, MSi-40, MSi-45 and MSi-50, respectively. This improvement can be because of the presence of CNT and nanostructures in the matrix. The mechanical properties of the final nanocomposite depend on the SiC formation, CNT amount and also

Table 4. Three-point Flexural test results of Strength of samples after heating at 1500°C

Specimens	Average (MPa)	Variation (%)	Test 1 (MPa)	Test 2 (MPa)	Test 3 (MPa)
MSi-00	52.10	0	55.43	58.20	42.68
MSi-30	72.42	+39	72.62	75.17	69.48
MSi-35	77.49	+48	73.59	81.48	77.41
MSi-40	81.14	+55	83.66	81.49	78.28
MSi-45	88.62	+70	88.04	92.54	85.29
MSi-50	83.26	+60	84.92	78.15	86.72

interactions of SiC, CNT and carbon matrix that are very complicated and need very deep investigations of micro and nano structures of material. These results are very similar to the curve of density of samples. This similarity can be a simple way to check the formation of ceramic matrix based on the density of samples.

Improvement of mechanical properties in final nanocomposite is related to the reaction of carbon matrix with Si particles, percentage of Si particles and nano structures in the matrix. The effect of nano structure is not investigated individually but rather in the scope of this research, it is observable that these nano structures are created in the matrix and can have huge enhancement of composite properties.

In this research, the main purpose is to indicate the nano structure formation in the presence of Si and carbon matrix, processing parameters and also nanostructures different morphologies.

4. Conclusion

In this article, a systematic procedure and experiment is conducted to determine the mechanical properties of Si/phenolic composites and also, processing of SiC and CNT in-situ formation in the matrix. Main achievement of this research is that it shows a new way for in-situ synthesis of nanocomposite with improved properties. The results show that hot-pressing of carbonized samples at 1500°C, can cause formation of SiC matrix and moreover, creation of some nanostructures in the matrix.

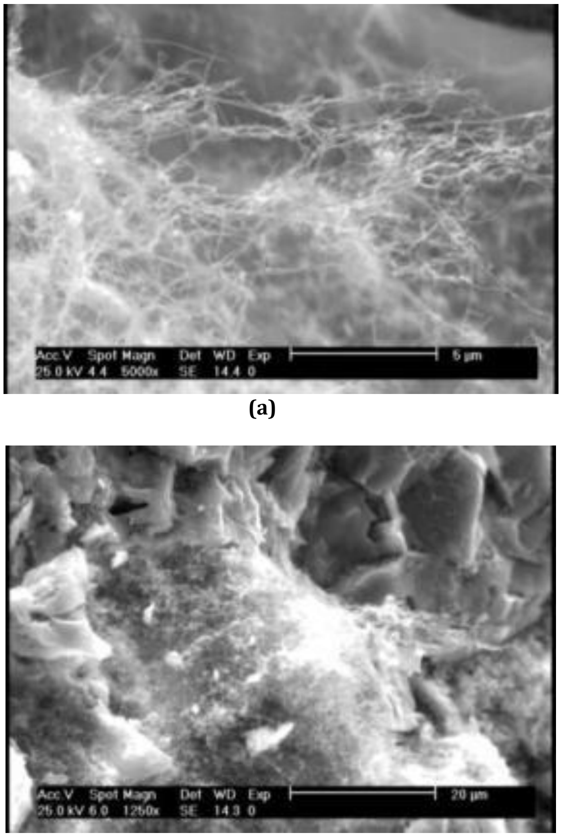

(a)

(b)

Figure 11. a) Formation of CNT in the presence of Si particles (5000X) **b)** Formation of CNT in the presence of Si particles (1250X)

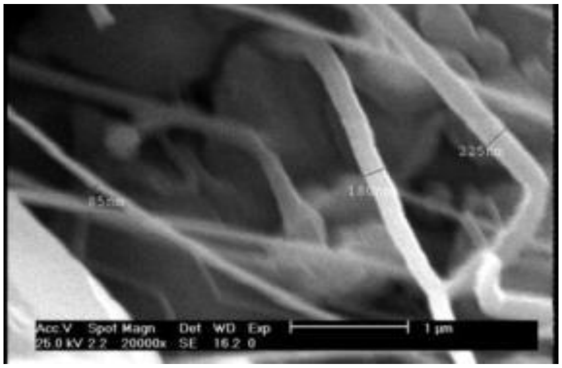

Figure 12. CNT dimension and diameter have been measured by SEM image

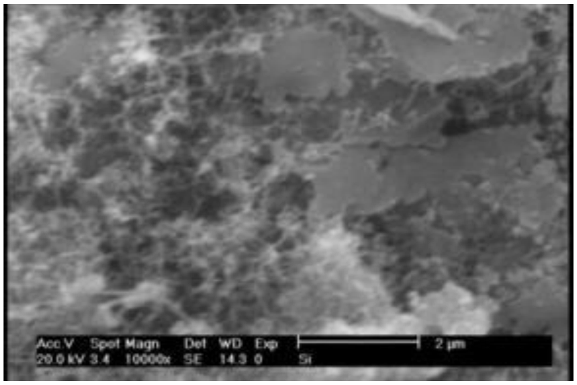

Figure 13. Formation of some plate-shaped nanostructures in the matrix

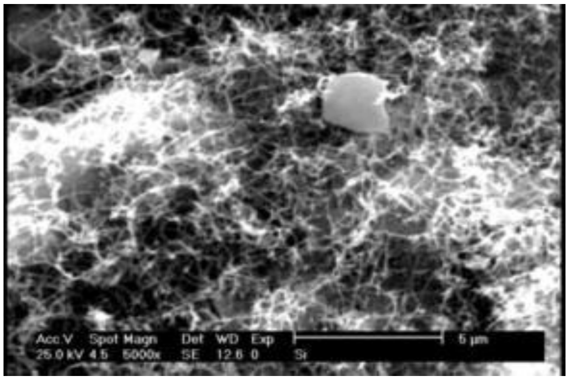

Figure 14. Growing of CNT in the SiC matrix

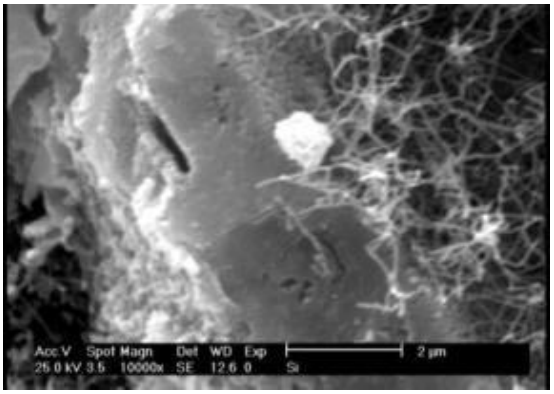

Figure 15. Agglomeration CNT sphere-shaped Structures in the matrix

These nanostructures are mainly grown because of presence of vaporized carbon atoms beside the Si catalyst particles that cause formation of CNT in the porosity of the matrix. The results of density and strength of samples show that the formation of SiC matrix is maximized in the sample MSi-45 that is also accompanied with better formation of CNT in the matrix.

References

[1] Fitzer E, Manocha LM. Carbon Reinforcements and C/C Composites. Springer, 1998.

[2] Fitzer E. The Future of the Carbon/Carbon Composites. Carbon 1987; 25: 163–190.

[3] Windhorst T, Blount G. Carbon/Carbon Composites; a Summary of Recent Developments and Applications. Mater Des 1997; 18: 11–15.

[4] Buckley JD. Carbon-Carbon, an Overview, Ceramic Bulletin 1988; 67(2): 364–368.

[5] Couzi J, DeWinne J, Leroy B. Improvements in Ablation Predictions for Reentry Vehicle Nosetip, in: W. Berry, J. Maylaert (Eds.). Proceedings of the Third European Symposium on Aerothermodynamics for Space Vehicles, 1998. p. 493–499.

[6] Trick KA, Saliba TE. Mechanisms of the Pyrolysis of Phenolic Resin in a Carbon/Phenolic Composite. Carbon 1995; 33(11): 1509-1515.

[7] Tzeng SS, Chr YG. Evolution of Microstructure and Properties of Phenolic Resin-Based Carbon/Carbon Composites During Pyrolysis. Mater Chem Phys 2002; 73(2-3): 162-169.

[8] Atarian M, Salehi HR, Atarian M, Shokuhfar A. Effect of oxide and carbide nanoparticles on tribological properties of phenolic-based nanocomposites. Iran Polym J 2012; 21(5): 297-305.

[9] Salehi HR, Khalili SMR. Thermal, Mechanical and Carbonization Behavior of High Temperature Phenolic Polymer. Adv Mater Eng 2011; 30(2): 69-81.

[10] Salehi HR, Salami S, Atarian M, Ozhdelnia O. Fabrication and Characterization of Pyrolyzed Phenolic/Carbon Nanocomposite and Reinforce it by Metal Oxide Nanoparticles. Adv Mater Eng 2013; 32(1): 39-53.

[11] Zawrah MF, Aly MH. In situ formation of Al2O3–SiC–mullite from Al-matrix composites. Ceramics Int 2006; 32(1): 21–28.

[12] D'angelo M, Deokar G, Steydli S, Pongrácz A, Pécz B, Silly MG, Sirottid F, Cavellin CD. In-situ formation of SiC nanocrystals by high temperature annealing of SiO2/Si under CO: A photoemission study. Surf Sci 2012; 606(7-8): 697–701.

[13] Jayaseelan DD, Zapata-Solvas E, Brown P, Lee WE. In situ Formation of Oxidation Resistant Refractory Coatings on SiC-Reinforced ZrB_2 Ultra High Temperature Ceramics. American Ceramic Soci 2012; 95(4): 1247–1254.

[14] Chung CK, Wu BH. Effect of substrate temperature on the in-situ formation of crystalline SiC nanostructured film using ultra-high-vacuum ion beam sputtering. Nanosci Nanotechnol 2010; 10(7): 4679-83.

[15] Wu B, Reddy RG. In-situ formation of SiC-reinforced Al-Si alloy composites using methane gas mixtures. Metal Mater Trans B 2002; 33(4): 543-550.

[16] Krishnarao RV, Ramarao VV, Mahajan YR. In situ formation of MoSi2–SiC through reaction of SiO2 or Si3N4 with Mo and carbon. Mater Res 1997; 12(12): 3322-3327.

[17] Oida S, Hannon JB, Tromp RM, McFeely FR, Yurkas J. A simple in situ method to detect graphene formation at SiC surfaces. Appl Phys Lett 2011; 98: 213106.

[18] Zhang GJ, Yue XM, Watanabe T, Yagishita O. In situ synthesis of Mo(Si,Al)2-SiC composites. Mater Sci 2000; 35(18): 4729-4733.

[19] Sun K, Yu J, Zhang C, Zhou X. In situ growth carbon nanotube reinforced SiCf/SiC composite. Mater Lett 2012; 66(1): 92–95.

[20] Salehi, HR. Synthesis and characterization of high temperature nanocomposite. MS thesis, Department of Mechanical Engineering, K. N. Toosi University of Technology, Tehran, Iran, 2009.

[21] ASTM Standard D790, 2010, Standard Test Methods for Flexural Properties of Unreinforced and Reinforced Plastics and Electrical Insulating Materials, ASTM International, West Conshohocken, PA, DOI: 10.1520/D0790-10, www.astm.org.

[22] ASTM Standard D792, 2008, Standard Test Methods for Density and Specific Gravity (Relative Density) of Plastics by Displacement, ASTM

International, West Conshohocken, PA, DOI: 10.1520/D0792-08, www.astm.org.